Gondwana Geological Magazine
Special Volume No.13, 2012, pp.1-14

GGM
www.ggsnagpur.org

Geochemistry of Uraniferous Banganapalle Sediments in the Western Part of Palnad Sub-basin, Andhra Pradesh: Implications on Provenance and Paleo-weathering

Shekhar Gupta, Rahul Banerjee*, P.V. Ramesh Babu, P.S. Parihar and P.B. Maithani

Atomic Minerals Directorate for Exploration and Research
1-10-153/156, AMD Complex, Begumpet, Hyderabad - 500 016
**E-mail: rahulbnrg@gmail.com*

Abstract

Banganapalle Formation (Kurnool Group) comprises intercalated arenaceous and argillaceous lithofacies with a basal conglomerate unit. Geochemically, basal conglomerate unit shows wide variation in major oxide contents due to the presence of polymictic clasts of diverse composition, *viz.* quartzite, shale, granite and vein quartz. Quartz arenites are highly mature (CMI: >10) as indicated by negative correlation between SiO_2 and Al_2O_3, MgO, K_2O and Na_2O. The argillaceous lithofacies (shale) contains significant amount of sulphide minerals and carbonaceous matter and higher concentration of trace elements *viz.*, Cr, Ni, Ba, Zr and Nb as compared to arenites. Major element distribution pattern, CIA values and discriminant function plots of these lithounits suggest that Banganapalle sediments were mainly derived from two different sources i.e., basement granitoids and quartzose Cuddapah sediments in passive margin setup. Uranium mineralisation in the area is fracture controlled and has no direct bearing with the geochemistry of sediments. Porous and permeable quartz arenites and the basal conglomerates with reductants in the form of sulphides and carbonaceous matter are best suited loci for uranium mineralisation.

Keywords : Palnad sub-basin, Banganapalle Formation, geochemistry, chemical index of alteration (CIA), provenance, paleo-weathering, uranium mineralization.

Introduction

The Palnad sub-basin extends over 3400 sq km in the northern part of Cuddapah basin and comprises arenaceous, argillaceous and carbonate sequences belonging to Kurnool Group (Nagaraja Rao *et al.,* 1987; Ramam and Murty, 1997; Saha and Chakraborty, 2003; Ramakrishnan and Vaidyanadhan, 2008). These sediments are widely studied by several geoscientists covering various aspects *viz.* stratigraphy, geochronology, structure, sedimentation pattern and depositional environment (Crawford and Compston, 1973; Dutt, 1975; Natarajan and Rajgopalan Nair, 1977; Nagaraja Rao *et al.,* 1987; Naqvi *et al.,* 1988; Lakshminarayana *et al.,* 2001; Saha and Chakraborty 2003; Gupta *et al.,* 2010). The Neoproterozoic Banganapalle Formation, which forms the base of the Kurnool Group, has shown immense economic potential particularly for diamond in conglomerate horizons (Vijayam and Reddy, 1976; Sivaji and Rao, 1989; Lakshminarayana *et al.,* 1999) and uranium in conglomerate and arenite horizons (Jeyagopal *et al.,* 1996, 2011; Nageswara Rao *et al.,* 2005; Basu *et al.,* 2008; Gupta *et al.,* 2009; Verma *et al.,* 2011).

The chemical composition of sediments is a function of its provenance, degree of weathering, transportation, sorting, diagenesis and tectonism (Bhatia, 1983; Roser and Korsch, 1986, 1988; Suttner and Dutta, 1986; Nesbitt and Young, 1989; Fedo *et al.,* 1995, 1997a, 1997b; Raza *et al.,* 2002; Wanders *et al.,* 2004). The lithogeochemical haloes and mineralogical alterations in sediments due to hydrothermal solutions are important tools to identify concealed unconformity-related uranium deposits (Sopuck *et al.,* 1983; Clark, 1987). Considering these factors, an attempt has been made in present paper for geochemical characterization of different lithofacies of Banganapalle Formation in western part of the Palnad sub-basin, Guntur district, Andhra Pradesh. Besides, provenance, paleo-weathering conditions and implication on uranium mineralisation in Banganapalle Formation have been discussed in the light of geochemical attributes in conjunction with petromineralogical observations.

Geological Set up

Meso- to Neo-proterozoic sediments of Cuddapah Supergroup and Kurnool Group are exposed in the northern part of crescent-shaped Cuddapah basin. These sediments rest unconformably over Archaean to Palaeoproterozoic basement granite and gneisses with younger intrusive granitoids and mafic rocks (GSI, 1981, 2001). Cuddapah sediments predominantly consist of arenaceous and argillaceous rocks with subordinate calcareous units whereas the Kurnool sediments are dominated by calcareous rocks with minor arenaceous and argillaceous sequences. In the Palnad sub-basin, Kurnool sediments unconformably overlie the older Cuddapah sediments in the eastern part whereas older granitoids form basement in the north and west. The Kurnool sequence begins with Banganapalle Formation, followed by Narji, Auk shale, Paniam, Koilkuntla and the uppermost Nandyal formation. A generalized lithostratigraphic succession of Cuddapah basin after Nagaraja Rao *et al.,* (1987) and Ramakrishnan and Vaidyanadhan (2008) is given in Table 1.

The study area (Koppunuru-Chenchu Colony and adjoining parts; 16°28'30"-16°32'00" : 79°18'00"-79°21'00"; T.S. Nos. 56 P/6 and 7) is marked by a yoked basin configuration where Palaeoproterozoic biotite granite are exposed as two inliers (Fig.1), one to the east of Koppunuru (6 km x 2 km; EW x NS) and the other, relatively smaller inlier, to the west of Chenchu Colony. These inliers represent basement highs in the eastern and western part of the study area, whereas in the southern sector, granites are exposed along the up-thrown block of WNW-ESE trending post Kurnool fault (Kandlagunta Fault). This fault is further offset by younger N-S trending faults. The basement granitoids are

Table 1: Generalised lithostratigraphic succession of Cuddapah basin.

Supergroup/Group/Subgroup		Formation	Thickness (m)
	Kundair	Nandyal Shale	50-100
	Subgroup	Koilkuntla Limestone	15-50
		Paniam Quartzite	10-35
Kurnool	~~~~~~~~~~ Paraconformity ~~~~~~~~~~		
Group	Jammalamadgu	Auk (Owk) Shale	10-15
	Subgroup	Narji Limestone	100-200
		Banganapalle Quartzite	10-50
~~ Unconformity ~~~~~~~~~~~~~~~~~~~~			
		Srisailam Quartzite	300
	~~ Unconformity ~~~~~~~~~~~~~~		
	Nallamalai Group	Cumbum Formation	2000
		Bairenkonda Quartzite	1500-4000
	~~ Angular Unconformity ~~~~~~~~~~		
Cuddapah	Chitravati Group	Gandikota Quartzite	330
Supergroup		Tadpatri Formation	4600
		Pulivendla Quartzite	1-75
	~~ Disconformity ~~~~~~~~~~		
	Papaghni Group	Vempalle Limestone	1900
		Gulcheru Quartzite	28-210
~~ Nonconformity ~~~~~~~~~~~~~~~~~~~~~~			
Archaean and Dharwars		Intrusive grey, medium grained, chloritised biotite granite gneisses/greenstones	

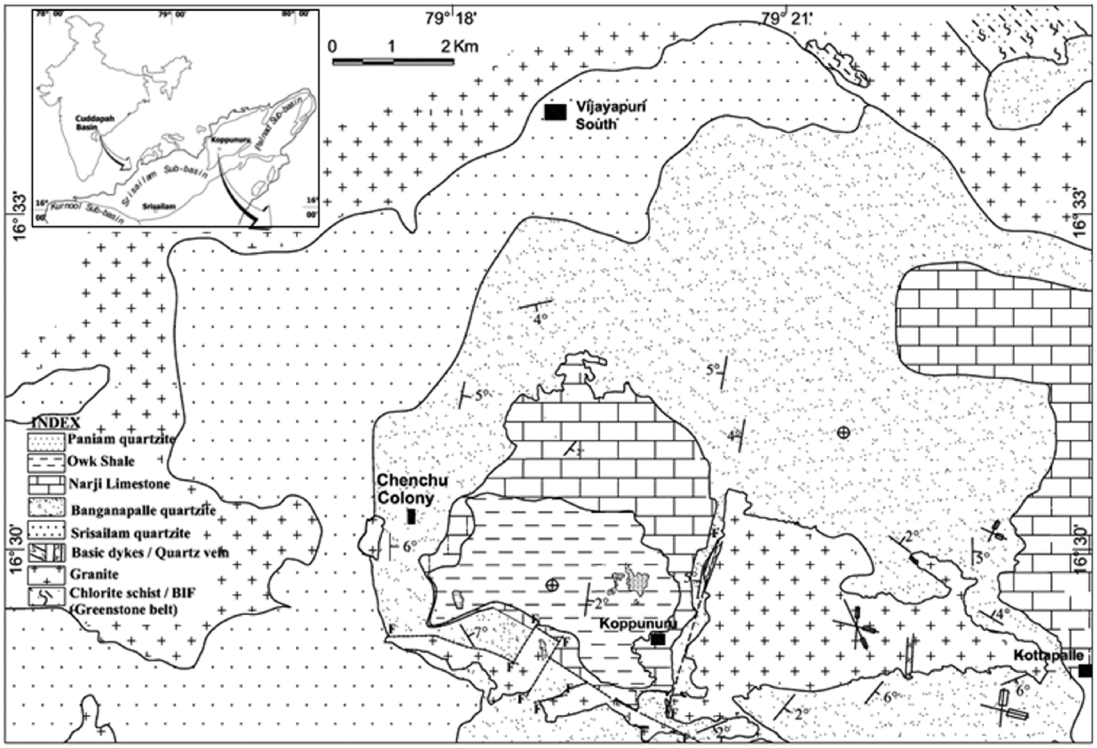

Fig.1. Geological map of the area around Koppunuru, western part of Palnad Sub-basin, Guntur district, Andhra Pradesh

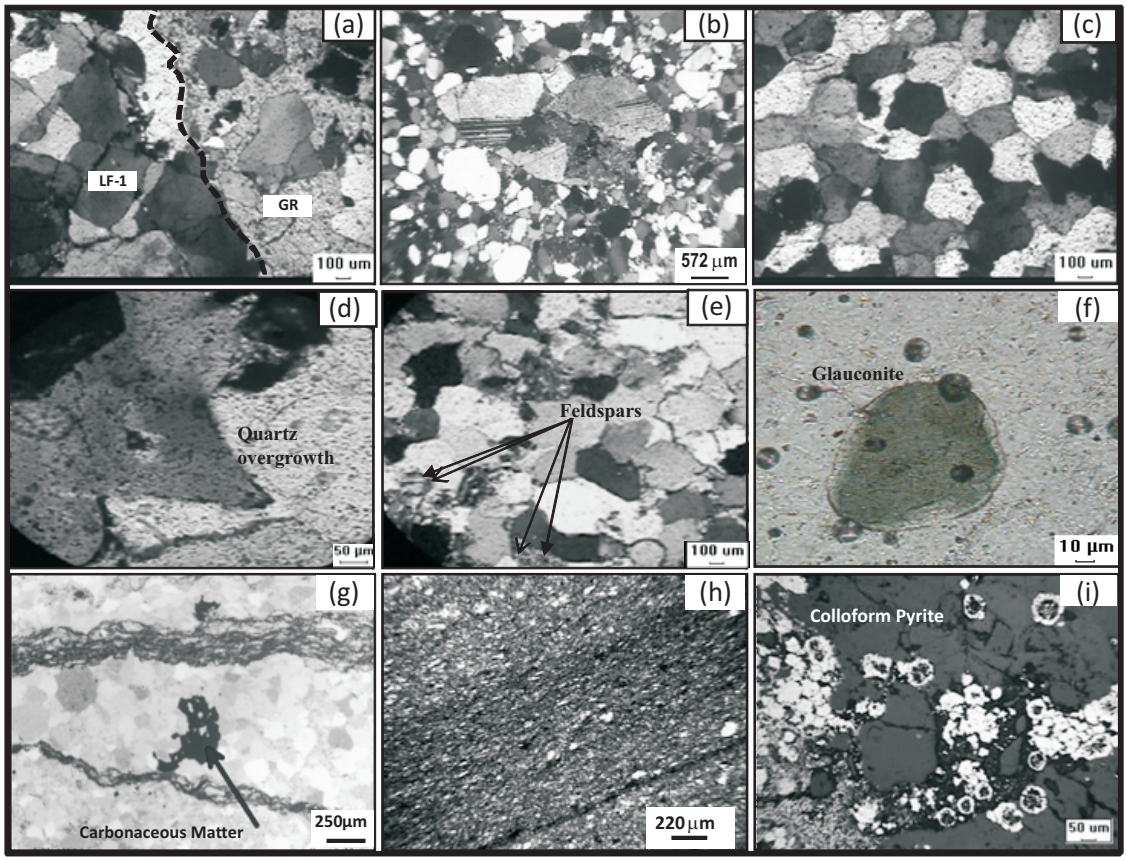

Fig.2. Photomicrograph showing **(a)** non-conformitycontact (dashedline) between granite (GR) and gritty-pebbly horizon (LF- 1); **(b)** poorly sorted nature and compositional variation in gritty- pebbly horizon; **(c)** well sorted and matured quartz grains in quartz arenite unit; **(d)** quartz grain showing secondary overgrowth; **(e)** feldspar grains is quartz arenite; **(f)** glauconite grainin quartz arenite; **(g)** carbonaceous matter in quartz arenite withthin laminations of shale; **(h)** argillaceous- arenaceous interlayerings in shale; **(i)** colloform/ framboidal pyrite and amorphous carbon in shale.

highly fractured and profusely traversed by dolerite dykes and quartz veins. These are unconformably overlain by sub-horizontal beds of Palnad (Kurnool) sediments (Fig.1). The overall thickness of the Palnad sediments in this part varies from 10m to 205m and dips are gentle (3-5°).

The Banganapalle Formation exposes monotonous sequence of quartz arenite (upper unit) in the study area, mostly due to sub-horizontal dips. Recent studies on lithofacies variation, sedimentation pattern and depositional environment of Banganapalle Formation based on borehole lithologs (Gupta *et al.,* 2010) have delineated five correlatable lithofacies deposited in inter- to supra-tidal flat tectono-sedimentary environment under stable shelf condition *viz.*, basal conglomerate (LF-1), quartzite-shale intercalations (LF-2), lower quartz arenite (LF-3), shale-siltstone intercalation (LF-4) and upper quartz arenite (LF-5). Thickness of Banganapalle sequence varies from 10m to 120m, which is mostly controlled by the basement topography.

Petrography

The basal conglomerate unit is represented by polymictic, poorly sorted, immature, grit to pebble size clasts, with minor grey to greenish grey shale intercalations and show close similarity with pebble bearing quartz arenite (Latha *et al.,* 2008, 2010). However, presence of pebbles (~60% of the rock volume) of various compositions such as granite, shale, quartzite, vein quartz, quartz arenite, altered feldspar and quartz of granitic origin and basic rock (at places) differentiates this unit from quartz arenite (Fig.2a and b). The interstitial material consists of subrounded quartz and feldspar clasts bound by predominantly sericitic matrix with minor chlorite. Framboidal and anhedral pyrite occurs as disseminations, intergranular fracture fillings and at places as segregation along pebble margins.

The quartz arenites are light grey in colour, medium to fine grained, well sorted and saccharoidal in nature. These are composed of unimodal, rounded to sub-rounded framework clasts of 0.2mm to 0.4mm size. The framework clasts account for ~90% of the rock by volume and are dominated by quartz (~97%; Fig.2c). The quartz is mainly monocrystalline in nature with a few grains of polycrystalline quartz. Modification of originally rounded quartz clast by secondary overgrowths is common (Fig.2d). Overgrown quartz is often welded by authigenic quartz into a mosaic of interlocking sutured aggregates. Other minor minerals include feldspars,

biotite, chlorite, sericite and chert. Feldspars are represented mainly by microcline, orthoclase and perthite (Fig.2e). Besides, glauconite is conspicuous in quartz arenite indicating reducing depositional environments (Fig.2f) while other ore minerals *viz.,* pyrite, anatase, xenotime, goethite, leucoxene and limonite form part of accessory minerals. Occasional thin laminations of shale and rounded aggregates of carbonaceous matter are also seen associated with quartz arenite (Fig.2g). Ferrugination is common in quartz arenites and they also exhibit other alteration features such as silicification, chloritization and kaolinization leading to formation of clay minerals *viz.,* illite and kaolinite. High degree of mineralogical and textural maturity indicates their deposition under high energy index in shallow marine conditions.

Shales are dark grey in colour, sub horizontally beded and show fine intercalations of light grey siltstone. Microscopically, they exhibit foliation defined by continuous, sub parallel sericite-rich bands (Fig.2h) alternating with granular arenaceous bands consisting of mainly quartz with minor microcline and plagioclase. At places, chlorite is associated with sericite. This facies is marked by the significant presence of sulphides and amorphous carbon. Pyrite is the major sulphide ore mineral and exhibits either colloform/framboidal nature (Fig.2i) or occurs as fine disseminations, thin stringers and veinlets.

Uranium mineralisation is mainly associated with conglomerate and quartz arenite units as fine veins, fractures/cavity fillings and along the grain boundaries. The primary uranium minerals identified are pitchblende and coffinite while variable concentration of uranium is also associated with sericitic clay, glauconite, chlorite, biotite and hydrated iron oxide. Presence of carbonaceous matter in mineralized horizons signifies its role as a reducing agent in fixation of the uraniferous lodes (Jeyagopal *et al.,* 2011).

Sampling and Analytical Method

A total of 71 core samples (conglomerate - 24 nos.; quartz arenite - 33 nos.; shale - 14 nos.) were collected from 27 boreholes spread over an area of 2.5 km (N-S) x 700m (E-W) in Koppunuru sector. During sampling proper care has been taken to collect pure fractions of quartz arenite and shale (without intercalations) while conglomerate contains mixed clasts and matrix.

The samples were analysed for major and trace elements using Philips X'unique II - WDXRFS (Wavelength Dispersive X-Ray Fluorescence Spectroscopy) controlled by computer with X-40 and Super Q software at XRF Laboratory, Atomic Minerals Directorate for Exploration & Research (AMD), Nagpur. The GFPC and SD detector based instrument consists of LiF220, 200, Ge, PET, TLAP, PX-1 and PX-4 crystal assembly and uses Rh target as a source of primary radiation. Overall precision and accuracy, as determined by replicate analyses, are estimated 2-5% (RSD) for major elements with >0.5% concentrations whereas 5% (RSD) for trace elements with >50 ppm and 10% (RSD) for <50 ppm concentrations.

Geochemistry

Analytical results of Banganapalle sediments show wide scatter in major and trace element distribution patterns of different lithounits (Table 2). Lithounitwise brief details of analytical results are discussed below.

Conglomerate

This unit is characterized by wide spread in SiO_2 (64.92-97.97 wt.%; av. 82.42 wt.%), Al_2O_3 (0.39-17.7wt. %; av. 7.91 wt. %) and FeO^t (0.09-5.98 wt. %; av. 1.51 wt. %) and are moderately rich in K_2O (0.15-6.63 wt. %; av. 2.8 wt. %), Na_2O (<0.01-2.29 wt. %; av. 1.03 wt. %) (Table 2). These conglomerates are poor in MgO (0.14-1.58 wt. %; av. 0.58 wt. %), MnO (<0.01-0.09 wt. %; av. 0.01wt. %), CaO (0.02-0.58 wt. %; av. 0.14 wt. %) and TiO_2 (<0.01-1.09 wt. %; av. 0.19 wt. %). The wide variation in major oxide compositions may be related to the presence of polymictic clasts of different composition as already discussed earlier. This is also depicted in major element based chemical classification diagram (Herron, 1988), where they straddle in the fields of sub-arkose, shale, wacke and sublithic arenite signifying the diversity in composition. Positive correlations of K_2O (r = 0.95), FeO^t (r = 0.70), MgO (r = 0.63) and TiO_2 (r = 0.64) with Al_2O_3 (Table 3) imply that clay minerals (illite, chlorite) and altered mica are the main phases controlling their distribution. As compared to Proterozoic equivalents (Condie, 1993), the conglomerate of Banganapalle Formation are enriched in U, Th, Rb, Pb and Y and depleted in Cr, Ba, Sr and Zr.

Quartz Arenite/Quartzite

Synthesis of major element data of quartz arenite/quartzite indicates higher SiO_2 content (81.30-99.22 wt. %, av. 92.18 wt. %), which is commensurate with comparatively low average Al_2O_3 (<0.01-7.61 wt. %; av. 2.25 wt. %) and FeO^t (0.46-7.34 wt. %; av. 2.81 wt. %) contents (Table 2). Besides, average content of other major oxides is low to very low (MgO: 0.51 wt. %; MnO: 0.01 wt. %; K_2O: 0.30 wt.%; Na_2O: 0.22 wt. %; TiO_2: 0.09 wt. %; CaO: 0.08 wt. %). Chemical classification of sandstone based on log (SiO_2/Al_2O_3), and log (Fe_2O_3/K_2O) ratios and CaO (Herron, 1988) indicates that arenaceous rocks of study area belong to quartz arenite and Fe-sand (Fig.3). The use of chemical log data is helpful in minimizing the influence of tectonic setting, depositional environment and source material (Pettijohn *et al.,* 1972), which results in close match of chemical and petrographic categorization of sediments. This observation also holds true for the quartz arenites of present study area.

Table 2: Major oxide (wt.%) and Trace element (ppm) data of Banganapalle Formation, western part of Palnad Sub-basin, Andhra Pradesh

Sample No.	PC-1	PC-2	PC-3	PC-4	PC-5	PC-6	PC-7	PC-8	PC -9	PC-10	PC-11	PC-12	PC-13	PC-14	PC-15	PC-16	PC-17	PC-18	PC-19	PC-20	PC-21	PC-22	PC-23	PC-24
												Conglomerate												
SiO_2	97.97	86.95	86.99	69.00	92.36	91.68	88.13	70.36	66.84	64.92	84.24	89.94	81.91	76.45	65.88	66.97	94.84	94.68	97.19	89.25	74.59	71.91	97.63	77.42
TiO_2	0.02	0.02	0.31	0.26	0.02	0.02	0.03	1.09	0.77	0.25	0.11	0.04	0.12	0.07	0.22	0.25	0.01	0.02	0.01	0.08	0.22	0.24	0.01	0.26
Al_2O_3	0.39	5.18	5.20	17.70	2.66	2.79	4.07	14.43	16.11	17.24	6.17	4.36	7.56	10.14	15.64	14.66	1.76	2.44	1.61	4.54	11.37	12.61	1.45	9.66
FeO^t	0.92	1.06	1.76	3.09	0.80	2.34	0.58	5.98	3.19	3.27	0.47	0.24	1.59	1.11	1.63	1.64	0.49	0.27	0.09	0.40	1.54	2.60	0.10	1.08
MgO	0.18	0.51	0.36	0.69	0.14	0.41	0.22	1.58	0.96	0.64	0.69	0.37	0.76	0.89	0.59	0.62	0.39	0.27	0.29	0.55	0.68	1.10	0.17	0.83
MnO	<0.01	<0.01	<0.01	0.01	<0.01	<0.01	<0.01	0.09	0.01	0.02	<0.01	<0.01	0.01	0.01	0.01	0.01	0.01	<0.01	<0.01	<0.01	0.01	0.01	<0.01	0.01
CaO	0.17	0.08	0.24	0.08	0.03	0.04	0.02	0.56	0.10	0.58	0.07	0.08	0.36	0.11	0.09	0.12	0.05	0.04	0.03	0.06	0.14	0.07	0.04	0.31
Na_2O	<0.01	<0.01	0.07	1.31	0.58	0.49	0.84	1.43	0.89	2.29	1.13	1.53	0.91	2.18	2.25	1.86	0.68	0.83	0.59	1.15	1.07	1.28	0.57	0.66
K_2O	0.15	2.57	2.02	5.86	1.20	0.98	1.42	2.81	5.21	6.32	2.01	1.69	2.29	3.87	6.63	6.18	0.53	0.87	0.26	1.65	4.04	4.51	0.65	3.48
P_2O_5	0.13	0.04	0.18	0.01	<0.01	0.02	0.01	0.40	0.03	0.23	0.03	0.02	0.22	0.06	0.05	0.08	0.04	0.03	0.03	0.03	0.04	0.04	0.05	0.26
Total	99.93	96.41	97.13	98.01	97.79	98.77	95.32	98.73	94.11	95.76	94.92	98.27	95.73	94.89	92.99	92.39	98.80	99.45	100.10	97.71	93.70	94.37	100.67	93.97
SiO_2/Al_2O_3	251.21	16.79	16.73	3.90	34.72	32.86	21.65	4.88	4.15	3.77	13.65	20.63	10.83	7.54	4.21	4.57	53.89	38.80	60.37	19.66	6.56	5.70	67.33	8.01
K_2O/ Na_2O	30.00	514.00	28.86	4.47	2.07	2.00	1.69	1.97	5.85	2.76	1.78	1.10	2.52	1.78	2.95	3.32	0.78	1.05	0.44	1.43	3.78	3.52	1.14	5.27
K_2O/ Al_2O_3	0.38	0.50	0.39	0.33	0.45	0.35	0.35	0.19	0.32	0.37	0.33	0.39	0.30	0.38	0.42	0.42	0.30	0.36	0.16	0.36	0.36	0.36	0.45	0.36
CIA	44.85	63.83	65.51	67.19	53.55	58.99	57.93	69.24	68.86	59.65	59.72	49.26	62.02	55.98	58.62	59.53	49.67	50.62	55.20	54.52	64.03	63.93	45.83	64.08
Cr	43	39	46	39	34	33	38	54	169	72	50	39	25	45	41	71	37	30	40	47	72	83	31	79
Ni	3	9	37	8	5	5	5	33	34	25	5	5	83	12	5	5	5	5	5	5	14	10	5	5
Cu	12	7	8	5	5	5	19	54	15	12	10	5	5	22	5	26	5	5	5	5	21	5	5	5
Zn	5	4	5	10	5	5	5	40	58	33	5	5	33	17	11	155	5	14	5	5	74	40	5	5
Rb	5	17	107	260	61	50	81	51	151	151	117	87	44	95	313	154	39	5	35	87	5	193	5	139
Sr	5	12	28	33	14	7	10	19	25	84	17	27	35	69	90	100	14	16	5	30	68	48	14	35
Y	17	15	16	21	6	7	8	98	45	57	5	5	5	29	14	11	5	36	5	5	33	5	16	5
Zr	2	7	166	216	5	5	40	130	289	223	207	121	185	25	295	239	57	47	73	119	113	262	39	191
Nb	5	3	5	5	5	5	5	14	14	14	20	16	6	5	33	15	5	5	5	13	9	27	6	15
Ba	112	462	203	362	116	90	122	489	1292	559	197	226	484	423	524	637	116	179	87	233	508	431	193	346
Pb	288	172	101	23	16	7	5	297	55	147	38	25	391	423	45	317	17	296	14	16	344	40	132	26
Th	5	5	5	87	25	18	41	5	18	26	54	34	10	5	100	33	16	5	14	45	5	63	5	31
U	915	640	83	70	28	6	41	1898	666	841	35	23	586	1631	47	2689	10	2097	11	19	1532	38	872	19
/Th	183.00	128.00	16.60	0.80	1.12	0.33	1.00	379.60	37.00	32.35	0.65	0.68	58.60	326.20	0.47	81.48	0.63	419.40	0.79	0.42	306.40	0.60	174.40	0.61

Sample No.	QA-1	QA-2	QA-3	QA-4	QA-5	QA-6	QA-7	QA-8	QA-9	QA-10	QA-11	QA-12	QA-13	QA-14	QA-15	QA-16	QA-17	QA-18	QA-19	QA-20	QA-21	QA-22	QA-23	QA-24
												Quartz Arenite												
SiO_2	95.38	95.56	91.67	96.06	93.54	88.55	93.83	84.59	92.26	99.22	93.36	87.39	97.36	92.15	88.70	95.70	95.56	90.94	97.72	90.29	94.22	84.61	90.28	92.80
TiO_2	0.03	0.03	0.02	0.02	0.01	0.05	0.04	0.22	0.08	<0.01	0.04	0.11	0.02	0.01	0.13	0.06	<0.01	0.02	<0.01	0.10	0.02	0.25	0.10	0.03
Al_2O_3	0.04	0.05	4.63	1.12	1.24	4.23	1.22	5.54	2.05	<0.01	1.30	4.19	0.20	1.25	4.22	0.35	<0.01	1.58	<0.01	3.21	0.67	6.20	2.91	1.08
FeOt	2.16	2.01	0.78	0.75	1.02	2.43	3.60	6.54	2.41	0.70	2.93	7.34	1.19	4.16	4.38	2.65	0.60	1.27	1.13	2.71	1.61	5.90	5.63	5.53
MgO	0.06	0.25	0.23	0.12	0.07	0.46	0.33	1.06	0.33	0.10	0.46	1.06	0.21	0.62	0.83	0.20	0.06	0.10	0.11	0.51	0.26	0.93	0.73	0.33
MnO	0.01	<0.01	<0.01	<0.01	0.01	0.01	0.01	0.01	<0.01	<0.01	0.01	0.02	<0.01	0.01	0.01	0.01	<0.01	<0.01	0.01	0.01	<0.01	0.01	0.01	<0.01
CaO	0.08	0.08	0.08	0.08	0.10	0.37	0.08	0.05	0.07	0.04	0.02	0.05	0.01	0.46	0.05	0.02	0.01	0.01	0.01	0.06	0.40	0.06	0.01	0.02
Na_2O	0.37	0.35	0.44	0.39	0.60	1.64	0.66	<0.01	<0.01	<0.01	<0.01	<0.01	<0.01	0.25	0.32	<0.01	<0.01	0.01	0.01	0.38	<0.01	<0.01	<0.01	<0.01
K_2O	0.10	0.27	1.05	0.09	0.31	0.25	0.12	0.92	0.15	<0.01	0.15	0.35	0.03	0.01	0.78	<0.01	<0.01	0.17	<0.01	1.07	0.10	1.28	0.32	0.02
P_2O_5	<0.01	<0.01	<0.01	<0.01	0.11	<0.01	<0.01	0.03	0.10	0.05	0.01	0.03	0.03	<0.01	0.03	0.01	<0.01	<0.01	<0.01	0.03	0.30	0.02	<0.01	0.03
Total	98.23	98.60	98.90	98.63	97.01	97.99	99.89	98.96	97.45	100.11	98.28	100.54	99.05	98.92	99.45	99.00	96.23	94.10	98.99	98.37	97.58	99.26	99.99	99.84
SiO_2/Al_2O_3	2384.50	1911.20	19.80	85.77	75.44	20.93	76.91	15.27	45.00	19844.00	71.82	20.86	486.80	73.72	21.02	273.43	19112.00	57.56	19544.00	28.13	140.63	13.65	31.02	85.93
K_2O/Na_2O	0.27	0.77	2.39	0.23	0.52	0.15	0.18	184.00	30.00	1.00	30.00	70.00	6.00	0.04	2.44	1.00	1.00	17.00	0.50	2.82	20.00	256.00	64.00	4.00
K_2O/Al_2O_3	2.50	5.40	0.23	0.08	0.25	0.06	0.10	0.17	0.07	1.00	0.12	0.08	0.15	0.01	0.18	0.01	1.00	0.11	1.00	0.33	0.15	0.21	0.11	0.02
CIA	4.43	4.70	69.77	55.88	45.18	53.74	47.27	83.50	87.31	5.47	86.27	89.76	77.26	49.83	74.28	87.50	13.58	87.84	11.10	62.91	44.26	80.49	88.64	94.22
Cr	171	102	48	42	105	88	128	75	43	29	37	52	40	28	65	45	28	36	32	59	36	77	55	40
Ni	150	84	54	73	95	76	110	10	9	5	4	5	4	5	5	5	5	5	5	5	5	16	5	7
Cu	28	21	21	19	25	25	19	3	13	9	4	17	11	5	5	5	11	25	7	8	5	15	5	12
Zn	12	681	5	5	5	10	9	79	12	5	32	19	5	6	5	25	5	5	5	5	15	13	7	27
Rb	35	36	61	24	54	52	26	5	5	5	5	5	5	36	75	21	25	17	16	65	32	72	41	43
Sr	5	8	19	9	16	28	5	2	5	5	5	5	5	5	5	5	5	5	5	5	7	5	5	5
Y	5	6	14	5	5	5	5	26	102	27	45	72	49	6	9	6	7	5	7	8	12	8	5	5
Zr	38	48	45	41	35	51	51	80	62	2	9	37	19	5	77	5	5	11	5	14	5	44	15	8
Nb	7	12	5	5	5	5	5	7	21	5	2	9	6	5	5	5	5	5	5	5	5	5	5	5
Ba	25	76	105	25	25	117	66	123	52	43	42	101	43	5	83	17	5	32	5	88	22	101	33	5
Pb	16	32	10	36	37	34	40	164	1016	251	184	269	345	6	9	47	6	98	18	15	5	14	8	7
Th	100	44	81	5	78	73	26	5	5	5	5	5	5	29	46	5	23	5	10	17	29	23	23	36
U	47	24	53	64	14	5	5	878	4992	1457	1140	4193	2168	23	43	15	5	23	5	19	16	18	14	33
U/Th	0.47	0.55	0.65	12.80	0.18	0.07	0.19	175.60	998.40	291.40	228.00	838.60	433.60	0.79	0.93	3.00	0.22	4.60	0.50	1.12	0.55	0.78	0.61	0.92

Sample No.	QA-25	QA-26	QA-27	QA-28	QA-29	QA-30	QA-31	QA-32	QA-33	SH-1	SH-2	SH-3	SH-4	SH-5	SH-6	SH-7	SH-8	SH-9	SH-10	SH-11	SH-12	SH-13	SH-14
												Quartz Arenite Shale											
SiO_2	92.02	89.17	97.88	81.30	97.00	90.45	94.99	93.52	83.91	81.50	73.61	65.65	60.90	69.62	70.69	63.50	57.37	67.36	65.55	66.26	62.80	66.26	62.80
TiO_2	0.04	0.05	<0.01	0.30	0.08	0.12	0.10	0.09	0.30	0.24	0.55	0.68	0.99	0.72	0.37	0.88	0.87	0.66	0.79	0.69	0.81	0.69	0.81
Al_2O_3	2.25	2.97	<0.01	7.61	0.72	3.54	1.49	2.26	6.14	6.82	11.98	18.12	22.60	23.02	13.86	19.30	20.33	18.56	17.16	17.08	19.22	17.08	19.22
FeOt	3.53	5.87	1.55	4.04	0.46	1.93	1.18	1.58	3.04	9.17	10.98	8.17	7.94	5.98	4.06	5.33	7.96	4.02	3.96	5.46	5.51	5.46	5.51
MgO	0.57	0.82	0.18	1.37	0.55	1.03	0.95	1.24	0.79	1.40	1.36	1.52	1.25	0.93	0.88	1.04	1.31	1.35	0.72	1.00	0.81	1.00	0.81
MnO	<0.01	0.01	<0.01	0.01	0.01	0.01	0.02	0.02	0.01	0.02	0.03	0.02	0.02	0.01	0.01	0.01	0.03	0.01	0.02	0.01	0.01	0.01	0.01
CaO	0.01	0.03	0.04	0.05	0.10	0.05	0.07	0.06	0.10	0.04	0.08	0.10	0.07	0.08	0.08	0.08	0.08	0.14	0.27	0.09	0.13	0.09	0.13
Na_2O	<0.01	<0.01	<0.01	0.27	0.49	0.01	0.46	0.32	0.18	<0.01	<0.01	<0.01	<0.01	0.27	0.11	<0.01	1.13	0.02	0.79	0.77	0.26	0.77	0.26
K_2O	0.29	0.21	<0.01	1.00	<0.01	<0.01	<0.01	<0.01	0.93	0.78	1.69	4.18	6.60	7.27	4.18	5.86	5.55	5.16	6.10	5.24	6.26	5.24	6.26
P_2O_5	<0.01	<0.01	<0.01	0.05	0.14	0.08	0.05	0.05	0.06	0.03	0.02	0.07	0.05	<0.01	<0.01	0.02	0.03	0.03	0.04	0.04	0.07	0.04	0.07
Total	98.71	99.13	99.65	96.00	99.55	97.22	99.31	99.14	95.46	100.00	100.30	98.51	100.42	107.90	94.24	96.02	94.66	97.31	95.40	96.64	95.88	96.64	95.88
SiO_2/Al_2O_3	40.90	30.02	19576.00	10.68	134.72	25.55	63.75	41.38	13.67	11.95	6.14	3.62	2.69	3.02	5.10	3.29	2.82	3.63	3.82	3.88	3.27	3.88	3.27
K_2O/ Na_2O	58.00	42.00	1.00	3.70	0.01	0.50	0.01	0.02	5.17	156.00	338.00	836.00	1320.00	26.93	38.00	1172.00	4.91	258.00	7.72	6.81	24.08	6.81	24.08
K_2O/ Al_2O_3	0.13	0.07	1.00	0.13	0.01	0.00	0.00	0.00	0.15	0.11	0.14	0.23	0.29	0.32	0.30	0.30	0.27	0.28	0.36	0.31	0.33	0.31	0.33
CIA	86.86	91.10	5.47	82.47	42.02	96.91	62.62	77.91	80.53	88.05	85.80	79.35	75.64	73.13	74.08	74.82	71.73	75.96	67.15	70.63	72.09	70.63	72.09
Cr	35	34	42	95	57	62	208	149	53	87	35	144	243	122	88	208	211	163	36	63	70	63	70
Ni	5	6	5	23	11	43	13	39	5	13	5	29	44	10	30	56	56	33	37	38	46	38	46
Cu	5	5	5	5	34	5	15	55	5	25	9	38	11	8	9	17	17	11	24	22	19	22	19
Zn	5	21	5	59	15	380	59	61	21	168	19	43	78	21	26	35	43	36	39	26	27	26	27
Rb	35	33	23	162	5	5	5	223	5	5	6	88	239	206	122	175	229	175	229	212	274	212	274
Sr	5	5	5	5	5	5	5	18	5	5	5	5	5	16	12	5	10	25	22	18	17	18	17
Y	6	<5	5	80	66	72	109	110	46	184	26	42	19	19	9	26	16	15	16	10	5	10	5
Zr	5	5	5	100	45	56	74	226	52	123	123	180	143	297	160	221	174	233	302	309	606	309	606
Nb	5	5	5	5	5	5	5	16	5	30	19	16	22	18	11	16	5	33	21	22	35	22	35
Ba	24	25	5	317	85	140	78	722	109	276	297	591	518	655	511	574	443	410	993	372	450	372	450
Pb	10	5	5	706	482	533	768	486	165	1559	245	202	121	82	223	115	48	20	34	29	138	29	138
Th	17	22	25	5	5	5	5	5	5	5	9	11	17	16	5	12	5	10	18	38	69	38	69
U	10	10	5	4625	2977	3358	5786	2754	2333	10231	1332	476	203	207	161	66	21	5	13	17	75	17	75
U/Th	0.45	0.20	925.00	595.40	671.60	1157.20	550.80	466.60	2046.20	148.00	43.27	11.94	12.94	32.20	5.50	4.20	0.50	0.72	0.45	1.09	0.45	1.09	0.45

Table 3: Correlation matrix of major oxides and trace elements of conglomerate (n=24)

	SiO_2	TiO_2	Al_2O_3	FeOt	MgO	MnO	CaO	Na_20	K_2O	P_20_5	Cr	Ni	Rb	Sr	Y	Zr	Nb	Ba	Pb	Th
TiO_2	-0.62	1																		
Al_2O_3	-0.99	0.64	1																	
FeO^t	-0.68	0.84	0.70	1																
MgO	-0.65	0.64	0.63	0.71	1															
MnO	-0.34	0.69	0.34	0.75	0.74	1														
CaO	-0.15	0.07	0.11	0.29	0.50	0.55	1													
Na_20	-0.62	0.13	0.60	0.29	0.57	0.35	0.46	1												
K_2O	-0.95	0.43	0.95	0.50	0.42	0.08	-0.02	0.57	1											
P_20_5	-0.29	0.59	0.27	0.59	0.48	0.69	0.35	0.05	0.10	1										
Cr	-0.55	0.60	0.54	0.40	0.42	0.08	-0.01	0.10	0.48	0.08	1									
Ni	-0.27	0.41	0.26	0.39	0.28	0.20	0.04	-0.05	0.16	0.52	0.14	1								
Rb	-0.73	0.25	0.73	0.33	0.33	0.00	0.08	0.56	0.78	-0.06	0.28	-0.06	1							
Sr	-0.74	0.11	0.70	0.23	0.38	0.09	0.27	0.80	0.79	0.08	0.20	0.05	0.59	1						
Y	-0.45	0.78	0.49	0.75	0.48	0.72	0.12	0.22	0.31	0.57	0.31	0.29	-0.04	0.13	1					
Zr	-0.79	0.50	0.79	0.41	0.48	0.09	0.00	0.45	0.77	0.18	0.57	0.32	0.77	0.55	0.14	1				
Nb	-0.57	0.26	0.52	0.24	0.53	0.23	0.26	0.65	0.52	0.06	0.32	-0.11	0.69	0.58	0.02	0.71	1			
Ba	-0.77	0.64	0.76	0.50	0.48	0.14	-0.04	0.33	0.75	0.13	0.79	0.42	0.41	0.48	0.45	0.66	0.34	1		
Pb	-0.18	0.17	0.17	0.15	0.15	0.16	-0.11	0.07	0.16	0.34	-0.05	0.44	-0.32	0.28	0.43	-0.08	-0.24	0.27	1	
Th	-0.42	-0.07	0.42	0.10	0.28	0.03	0.32	0.61	0.45	-0.26	-0.02	-0.29	0.81	0.45	-0.26	0.50	0.70	0.07	-0.50	1
U	-0.27	0.32	0.27	0.22	0.15	0.25	-0.14	0.14	0.26	0.25	0.13	0.14	-0.24	0.32	0.57	-0.01	-0.15	0.35	0.84	-0.44

Low TiO_2 content in quartz arenite points to the negligible presence of phyllosilicate (Dabard, 1990; Condie *et al.,* 1992). Trace element distribution pattern has indicated enrichment of U and Th and depletion of Sr, Ti, Ba and Zr as compared to average upper crust composition, which closely resembles to the observations on Banganapalle quartzites by Karuppan *et al.* (2010). Uraniferous samples have shown depletion of Rb and Th while low uranium bearing samples show comparatively higher Rb and Th. Strong positive correlation (r = 0.95) between U and Y (Table 4) signify presence of some REE bearing resistate minerals in the system. Moderate negative correlation (r = -0.47) between U and Th, suggests that U is decoupled from Th and mobilised in the system due to it's highly oxyphile nature.

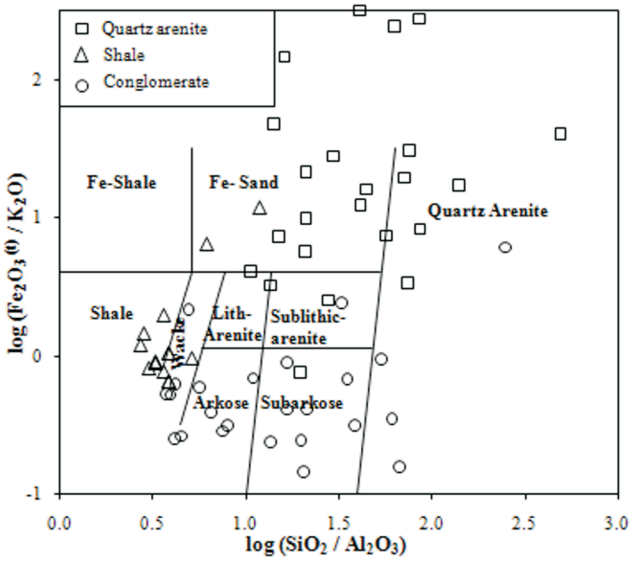

Fig.3. Chemical composition of arenaceous and argillaceous sediments of Banganapalle Formation and their classification as per sand class scheme (*after* Herron, 1988)

Very high content of SiO_2 *vis-à-vis* very high (>10) SiO_2/Al_2O_3 ratio (CMI, Potter, 1978) and negative correlation between SiO_2 and Al_2O_3 (r = - 0.87), K_2O (r = - 0.16), MgO (r = -0.40) and Na_2O (r = -0.09) indicate high chemical maturity of the arenites (Table 4). Besides, implication of climatic conditions on the chemical maturity has also been studied using bivariant plot of Suttner and Dutta (1986) *i.e.,* SiO_2 vs. Al_2O_3+ K_2O+ Na_2O diagram, which shows humid to sub-humid depositional paleoclimate for these siliciclastic sediments (Fig.4). Development of quartz arenites in tropical climates might have also played vital role in retention of oxyphile elements, such as uranium in the system.

Shale

The argillaceous facies is characterized by moderate to high SiO_2 (57.37-81.50 wt. %, av. 66.71wt. %), Al_2O_3 (6.82-23.02 wt. %, av. 17.45 wt. %), FeO^t (3.96-10.98 wt. %, av. 6.39 wt. %), K_2O (0.78-7.27 wt. %, av. 5.03 wt. %) and TiO_2 (0.24-0.99 wt. %, av. 0.70 wt. %), moderate MgO (0.72-1.52, 1.10 wt. %) and low Na_2O (0.01-1.13 wt. %, av. 0.31wt. %) and CaO (0.04-0.27 wt. %, av. 0.10 wt. %) (Table 2). High TiO_2 content indicate the higher content of phyllosillicate. These shale samples are enriched in Cr, Rb, Zr, Pb and U and exhibit depletion in Sr, Ba, Ni and Th. Concentration of trace elements *viz.* Cr, Ni, Ba, Zr and Nb are higher in shale than in quartz arenite and basal conglomerate, which can be attributed to the higher clay mineral content as well as some contribution from mafic rocks in the provenance. These samples predominantly fall in shale and wacke fields in Herron's chemical classification diagram (Fig.3).

Table 4: Correlation matrix of major oxides and trace elements of quartz arenites (n=33)

	SiO_2	TiO_2	Al_2O_3	FeOt	MgO	MnO	CaO	Na_2O	K_2O	P_2O_5	Cr	Ni	Cu	Zn	Rb	Sr	Y	Zr	Nb	Ba	Pb	Th
TiO_2	-0.77	1																				
Al_2O_3	-0.87	0.85	1																			
FeO^t	-0.68	0.48	0.54	1																		
MgO	-0.40	0.44	0.40	0.43	1																	
MnO	-0.24	0.34	0.28	0.29	0.16	1																
CaO	-0.07	-0.12	0.01	-0.04	-0.05	0.00	1															
Na_2O	-0.09	-0.06	0.12	-0.22	-0.12	0.19	0.46	1														
K_2O	-0.16	0.32	0.23	-0.04	0.12	0.05	-0.01	0.17	1													
P_2O_5	0.10	0.06	-0.05	-0.22	-0.02	-0.03	0.41	-0.06	0.26	1												
Cr	-0.04	0.19	0.06	-0.08	0.09	0.59	0.00	0.45	-0.03	-0.02	1											
Ni	0.16	-0.19	-0.13	-0.22	-0.12	0.02	0.13	0.58	-0.10	-0.12	0.59	1										
Cu	0.16	-0.18	-0.15	-0.34	-0.16	0.33	0.03	0.46	0.23	0.04	0.51	0.50	1									
Zn	0.19	0.04	-0.06	-0.06	0.06	-0.06	-0.05	0.00	-0.07	-0.02	0.19	0.26	0.05	1								
Rb	-0.33	0.27	0.35	0.06	-0.04	0.31	0.03	0.21	0.00	-0.02	0.34	0.14	0.45	-0.02	1							
Sr	-0.03	-0.20	0.12	-0.29	-0.17	0.10	0.38	0.75	-0.05	0.00	0.22	0.43	0.56	-0.01	0.41	1						
Y	-0.06	0.37	0.23	-0.06	0.09	0.56	-0.14	-0.08	0.15	0.27	0.35	-0.20	0.26	0.08	0.21	-0.03	1					
Zr	-0.26	0.43	0.39	0.00	0.27	0.56	-0.04	0.27	0.10	0.07	0.60	0.22	0.60	0.16	0.71	0.35	0.62	1				
Nb	0.00	0.03	-0.03	-0.01	0.06	0.14	-0.04	-0.05	-0.10	0.12	0.20	0.09	0.42	0.25	0.26	0.13	0.51	0.53	1			
Ba	-0.24	0.38	0.36	0.00	0.17	0.53	-0.04	0.16	0.07	0.06	0.42	0.07	0.58	0.11	0.82	0.37	0.58	0.92	0.44	1		
Pb	0.00	0.33	0.17	-0.15	0.07	0.32	-0.14	-0.05	0.16	0.29	0.30	-0.15	0.16	0.10	0.10	-0.10	0.93	0.49	0.53	0.40	1	
Th	0.00	-0.29	-0.05	-0.09	-0.19	-0.16	0.30	0.52	-0.07	-0.07	0.29	0.67	0.26	0.02	0.13	0.53	-0.47	-0.07	-0.09	-0.17	-0.45	1
U	-0.10	0.42	0.26	-0.03	0.08	0.49	-0.13	-0.07	0.16	0.26	0.32	-0.20	0.11	0.08	0.05	-0.14	0.95	0.47	0.41	0.39	0.94	-0.47

Discussion and Conclusions

Integrated studies of field geological, exploratory drilling, petromineralogical and geochemical data sets of Banganapalle Formation around Koppunuru-Chenchu colony area in parts of Guntur district, Andhra Pradesh, an important geological domain, reveals a complex evolutionary and mineralization history. The pre- and post- sedimentation magmatic and tectonic activities have led to large scale potash metasomatism of basement together with emplacement of highly evolved acid, alkaline and mafic intrusive *vis-à-vis* alteration of basement rocks/cover sediments. This has also influenced the sedimentation patterns and accelerated mobilisation of various elements including radioelements. The ideal geological setup for unconformity-related and/or fracture-controlled uranium mineralisation *i.e.*, Neoarchaean to Palaeoproterozoic basement complex and a thick pile of Neoproterozoic cover sediments (Banganapalle Formation) together with substantial structural disturbances in the form of major faults/ fractures has led to the formation of uranium deposit of economic significance at Koppunuru (Gupta *et al.,* 2009, 2010; Karuppan *et al.,* 2010; Jeyagopal *et al.,* 2011; Verma *et al.,* 2011).

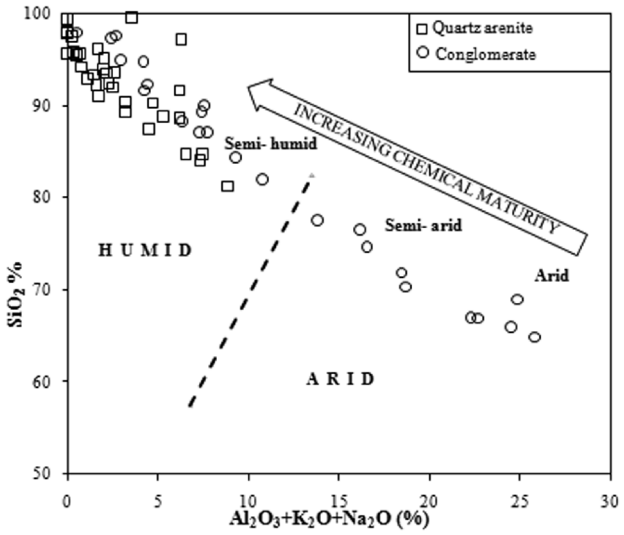

Fig.4. Chemical maturity of Banganapalle sediments expressed as function of SiO_2 %, and total $Al_2O_3 + K_2O + Na_2O$ % (*after* Suttner and Dutta, 1986).

An overall assessment and evaluation of geochemical data of Banganapalle sediments (n = 71) has indicated strong positive correlation (r = 0.95) between U and Pb (Table 5) indicating their radiogenic nature. Positive correlation of K_2O with Al_2O_3 (r = 0.96), TiO_2 (r = 0.76), Ba (r = 0.79) and Rb (r = 0.84) (Table 5) suggests that the concentration of these elements are mainly controlled by clay minerals. The K_2O/Al_2O_3 ratio, an important indicator to identify original composition of terrigenous sediments (clay minerals: 0-0.3; feldspars: 0.3-9.0; Cox *et al.,* 1995), has also indicated dominance of clay minerals (illite and chlorite) in quartz arenites and shale showing values <0.3 (34 samples) while most of the conglomerate samples (n=20) and remaining arenite/shale samples with higher K_2O/Al_2O_3 ratio (> 0.3) (Table 2) probably reflect input from first cycled granitic material (Nagarajan *et al.,* 2007). Presence of K-feldspar in these samples has also been corroborated by petrographic study. In addition, positive correlation of Ba with K_2O suggests that Ba is mainly associated with K-feldspars. Apart

Table 5: Correlation matrix of major oxides and trace elements of Banganapalle Formation (n=71)

	SiO_2	TiO_2	Al_2O_3	FeOt	MgO	MnO	CaO	Na_2O	K_2O	P_2O_5	Cr	Ni	Cu	Zn	Rb	Sr	Y	Zr	Nb	Ba	Pb	Th
TiO_2	-0.86	1																				
Al_2O_3	-0.98	0.88	1																			
FeOt	-0.56	0.63	0.53	1																		
MgO	-0.69	0.68	0.66	0.72	1																	
MnO	-0.37	0.54	0.34	0.46	0.57	1																
CaO	-0.27	0.22	0.24	0.04	0.16	0.46	1															
Na_2O	-0.36	0.03	0.33	-0.25	0.05	0.19	0.39	1														
K_2O	-0.94	0.76	0.96	0.34	0.48	0.20	0.23	0.44	1													
P_2O_5	-0.15	0.19	0.13	-0.05	0.17	0.50	0.74	0.22	0.12	1												
Cr	-0.42	0.50	0.45	0.35	0.48	0.22	-0.04	-0.04	0.36	-0.08	1											
Ni	-0.11	0.16	0.11	0.07	-0.02	0.10	0.18	0.07	0.08	0.03	0.48	1										
Cu	-0.20	0.30	0.18	0.15	0.27	0.54	0.22	0.16	0.11	0.24	0.32	0.41	1									
Zn	-0.01	0.00	-0.01	0.06	0.12	0.03	-0.04	-0.04	-0.02	-0.03	0.18	0.25	0.13	1								
Rb	-0.79	0.64	0.80	0.25	0.42	0.10	0.12	0.38	0.84	0.02	0.37	0.14	0.14	-0.05	1							
Sr	-0.45	0.05	0.41	-0.21	0.07	0.04	0.35	0.82	0.56	0.25	-0.06	-0.04	0.08	0.02	0.42	1						
Y	-0.01	0.08	-0.01	0.24	0.45	0.42	0.06	-0.08	-0.13	0.23	0.20	-0.11	0.38	0.19	-0.15	-0.08	1					
Zr	-0.78	0.70	0.79	0.31	0.46	0.15	0.19	0.28	0.80	0.14	0.27	0.18	0.21	0.02	0.83	0.37	-0.02	1				
Nb	-0.66	0.60	0.66	0.38	0.47	0.18	0.10	0.18	0.65	0.07	0.25	0.06	0.21	0.10	0.66	0.31	0.15	0.81	1			
Ba	-0.78	0.68	0.78	0.25	0.55	0.30	0.26	0.38	0.79	0.17	0.40	0.11	0.31	0.05	0.66	0.48	0.15	0.69	0.53	1		
Pb	0.03	-0.04	-0.05	0.14	0.33	0.19	-0.04	-0.10	-0.13	0.16	0.10	-0.08	0.24	0.21	-0.20	-0.02	0.88	-0.01	0.17	0.07	1	
Th	-0.16	-0.04	0.15	-0.10	-0.19	-0.16	0.06	0.38	0.23	-0.11	0.01	0.36	0.04	-0.02	0.43	0.29	-0.38	0.34	0.29	-0.01	-0.38	1
U	0.08	-0.08	-0.11	0.16	0.33	0.21	-0.08	-0.10	-0.20	0.11	0.10	-0.15	0.22	0.22	-0.25	-0.05	0.91	-0.08	0.11	0.01	0.95	-0.37

from this, an overall negative correlation of SiO_2 is quite apparent with most of the major oxides and some trace elements *viz.,* Rb, Ba and Zr (Table 4). The provenance signature in the chemistry of sediments also allows effective discrimination of tectonic environment at the time of sedimentation (Roser and Korsch, 1986). Based on this analogy, the Banganapalle sediments were subjected to tectonic discrimination plots using SiO_2, K_2O and Na_2O relationship, which broadly indicates their derivation in Passive Margin (PM) setup (Fig.5). This is corroborated by quartz-rich nature and deposition of these sediments in close proximity to the provenance. Various details pertaining to provenance, paleoweathering and uranium mineralisation are discussed in the following paragraphs.

Provenance

Sedimentological and other related aspects of the Banganapalle Formation were studied by various workers (Vijayam and Reddy, 1976; Sivaji and Rao, 1989; Lakshminarayana *et al.,* 1999; Gupta *et al.,* 2010) and envisaged shallow marine depositional environment with provenance comprising granites in the north and west while older Cuddapah sediments in the south and west. In the study area, the basal conglomerate of the Banganapalle Formation is marked by presence of poorly sorted angular to sub-angular clasts of mixed composition (both granitic and sedimentary). This indicates short distance transportation and derivation of sediments from nearby provenance. Apart from the basal conglomerate, the Banganapalle litho column is represented by cyclic repetition of arenaceous and argillaceous sediments which indicates alternate marine transgression and regression regimes together with shallow marine, inter-tidal flat depositional environment (Gupta *et al.,* 2010).

Geochemically, SiO_2/Al_2O_3 and K_2O/Na_2O ratios are known to indicate the provenance and the type of feldspars present in source rock (Naqvi *et al.,* 1988) as well as chemical maturity (CMI; SiO_2/Al_2O_3; Potter, 1978). SiO_2/Al_2O_3 ratio for conglomerate of study area (3.77-67.33; mean=20.05; except one sample, Table 2) indicate mainly a felsic provenance and suggest that these poorly sorted sediments were derived from the positive areas having granite in the north, east and west. In contrast, quartz arenites show CMI values >10 signifying a quartz-rich and highly mature nature.

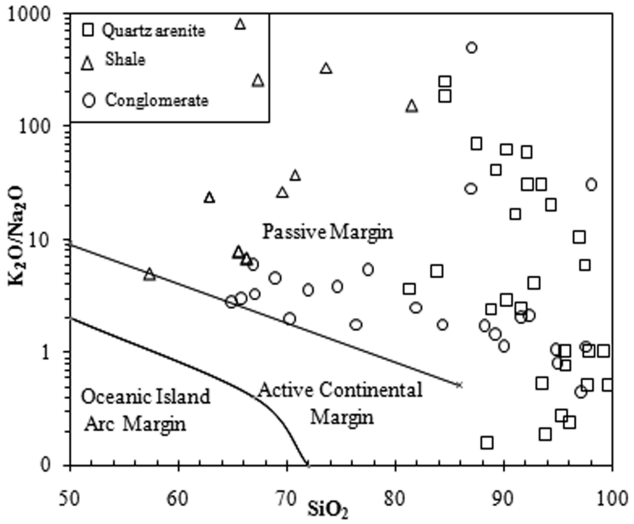

Fig.5. SiO_2 vs. K_2O / Na_2O discriminant diagram (*after* Roser and Korsch, 1986) showing deposition of Banganapalle sediments in a passive margin tectonic setting

On the basis of CMI values, these arenites can be grouped into three different classes *i.e.*, very high (1911-19844; n=6; 18%), high (64-487; n=11; 33%) and moderately high (10-57; n=16; 49%) maturity. This behaviour is in accordance with the presence of Upper Cuddapah quartzose sedimentary provenance in the west and south whereas in other sectors older granitic rocks with mafic intrusive mark the source area for the matured quartz arenites of Banganapalle Formation. Low SiO_2/Al_2O_3 ratio (2.69-11.95; mean=4.31) in shale is in accordance with substantial weathering of bed rocks yielding Al-rich sediments dominated by clay minerals.

K_2O/Na_2O ratio in sandstones is another important chemical parameter, which depends on both the composition of source and intensity of weathering (Lindsey, 1999). Besides, there is a tendency of increase in K_2O/Na_2O ratio with progressive weathering while total alkali content decreases due to the destruction of feldspars among which plagioclase is more preferentially removed than K-feldspars (Nesbitt and Young, 1984; Nesbitt *et al.,* 1996, 1997). In the studied Banganapalle quartz arenites, bimodal distribution of K_2O/Na_2O ratio was observed *i.e.,* (i) K_2O/Na_2O >1 with moderate SiO_2/Al_2O_3 (n= 18; 55%) suggesting a chemically weathered provenance with appreciable presence of K-feldspar and (ii) $K_2O/Na_2O \leq 1$ with moderate to high SiO_2/Al_2O_3 (n= 15; 45%) signifying relatively less weathered and quartz dominated matured provenance. In contrast, shales show very high K_2O/Na_2O ratio indicative of chemically weathered provenance while conglomerate/arenites exhibit wide fluctuation in K_2O/Na_2O ratio in accordance with their polymictic composition.

Discriminant function analysis using major oxides (*after* Roser and Korsch, 1986) were also attempted to identify provenance for Banganapalle sediments. Classification plot based on Discriminant function coefficients using TiO_2, Al_2O_3, $FeO^{(t)}$, MgO, Na_2O and K_2O *i.e.,* F1 and F2 scores (Fig.6) substantiates the dual source area *i.e.,* quartzose sedimentary as well as felsic igneous provenance as indicated also by K_2O/Na_2O and SiO_2/Al_2O_3 ratios.

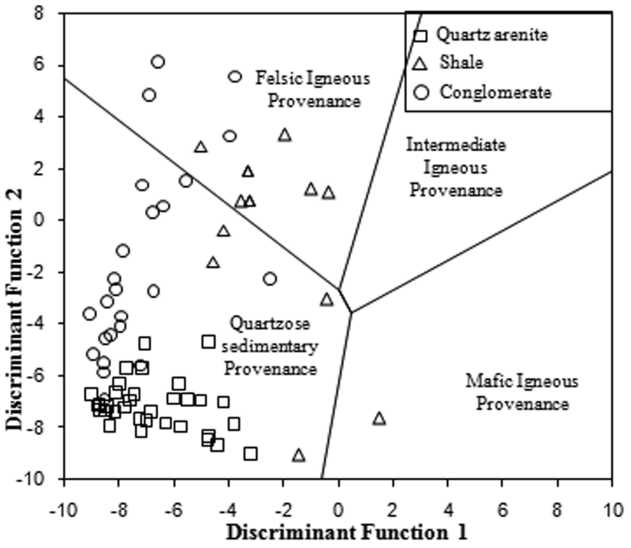

Fig.6. Discriminant Function Diagram for sedimentary provenance of Banganapalle Formation using major elements (*after* Roser and Korsch, 1988). The Discriminant Function 1 = (-1.7773*TiO_2) + (0.607*Al_2O_3) + (0.76*Fe_2O_3) + (-1.5*MgO) + (0.616*CaO) + (0.509*Na_2O) + (-1.224*K_2O) + (-9.09)
Discriminant Function 2 = (0.445*TiO_2) + (0.07*Al_2O_3) + (-0.25*Fe_2O_3) + (-1.142*MgO) + (0.438*CaO) + (1.475*Na_2O) + (1.426*K_2O) + (-6.861).

Paleo-weathering

Alterations of minerals in present day sediments are representative of the intensity and duration of chemical weathering processes operative in the source terrain. Chemical Index of Alteration (CIA) of derived clastic rock gives a quantitative measure of paleo-weathering conditions, and signifies the progressive weathering of feldspar to clay minerals (Fedo *et al.,* 1995; Armstrong-Altrin *et al.,* 2004). CIA is calculated using molecular proportion of elements present in clastic rocks as per the equation given by Nesbitt and Young (1982): CIA= [$Al_2O_3/(Al_2O_3+CaO^*+K_2O+Na_2O)$] x 100, where CaO* represent Ca in silicate fraction. High CIA values (76-100) indicate intensive chemical weathering in the source areas due to removal of labile cations (Ca^{2+}, Na^+, K^+) relative to stable residual constituent (Al^{3+}, Ti^{4+}) and yields mineral compositions trending towards kaolinite or gibbsite. In contrast, low CIA values (50 or less) suggest less weathered/unweathered source rock, negligible chemical alteration and cool/arid conditions (Nesbitt and Young, 1982; Fedo, 1995; Nagarajan *et al.,* 2007).

In the present study, total CaO was used for calculating CIA considering very low CaO content in most of the samples (Table 2). The CIA values of Banganapalle quartz arenites show wide scatter from 4.43 to 96.91 (av. 61.55), but distinct bi-modal CIA pattern is observed *i.e.,* 48.5% samples showing CIA >76 while remaining samples have low CIA ($\leq$50). This suggests that sediments are derived from two different provenances, one that has undergone intensive chemical weathering and the other relatively unweathered to moderately weathered. In contrast, Banganapalle shale with high CIA (67.15-88.05; mean 75.1), indicates substantial weathering in source terrain. The chemical weathering in source terrains for quartz arenites and shales are depicted by strong depletion of CaO, Na_2O and Sr. Conglomerate show CIA ranging from 44.85 to 68.24 (av. 58.44), suggestive of moderately weathered provenance.

The CIA values of Banganapalle sediments have also been evaluated by plotting the data in Al_2O_3-CaO*+Na_2O - K_2O (A-CN-K) compositional space (Nesbitt and Young, 1982, 1984; Fedo *et al.,* 1995) (Fig.7). Majority of the Banganapalle sediments cluster above the feldspar join line, except a few quartz arenite samples falling far below the feldspar join line and approach CN-apex indicating low Al_2O_3

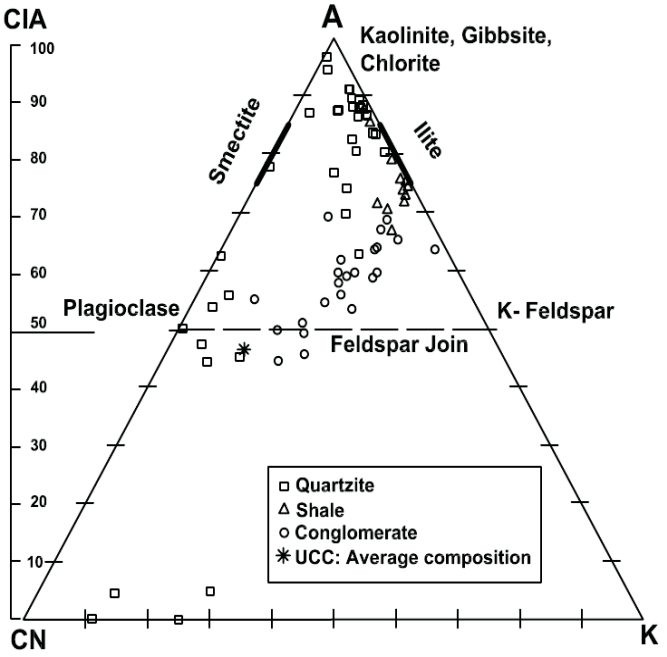

Fig.7. Molar Al_2O_3 - ($CaO+Na_2O$) + K_2O (A-CN-K) plots for Banganapalle sediments. UCC: Average composition of upper continental crust (Taylor and McLennan, 1985). CIA: Chemical Index of Alteration (Nesbitt and Young, 1982).

content and high chemical maturity. Quartz arenites are seen forming two distinct clusters *i.e.,* (i) plotting away from the feldspar join and approaching towards A-apex; though sample plots are scattered but broadly follow the A-K line trend signifying prior removal of Ca and Na in preference to Al and K during intensive chemical weathering in the source areas as well as impact of post-depositional potash metasomatism, and (ii) scattered near the feldspar join and sub-parallel to A-CN join suggestive of unweathered to moderately weathered source composition. Shale samples plot away from the feldspar join line and mostly straddle in the field of illite exhibiting a distinct trend sympathetic to A-K line. This behaviour not only indicates substantial weathering in the source area but also subsequent potash metasomatism of the sediments. Conglomerates are scattered near the feldspar join line and do not show any specific trend.

General abundance of K_2O in Banganapalle sediments is higher than the normal abundance pointing towards the possibility of metasomatic enrichment as also indicated by A-CN-K triangular diagram. An overall assessment of data has shown that 93% shales, 79% conglomerates and 15% quartz arenite contain higher K_2O as compared to the average compositions of cratonic shales and quartzite (Condie, 1993). Generally metasomatic enrichment of potassium brings mineralogical changes in original composition of sediments (Condie, 1993; Fedo *et al.,* 1997a) and it is mostly resulted due to the involvement of potassium bearing pore waters. Two major processes of potash metasomatism in siliciclastic sediments are identified by Fedo *et al.* (1995, 1997a) *viz.,* (i) conversion of kaolinite dominated clay minerals/matrix to illite, and (ii) conversion of plagioclase to potash feldspar. In the present study no significant petrographic evidences of replacement of plagioclase by potash feldspar were observed, but the presence of illite is confirmed by XRD. This is further substantiated geochemically by K_2O/Al_2O_3 ratio >0.18, indicating introduction of K in aluminous clays to form illite in sediments (Sopuck *et al.,* 1983; Fedo *et al.,* 1995).

Uranium Mineralisation

Banganapalle Formation in western part of Palnad sub-basin has shown immense potential of uranium mineralisation (130-5500ppm U_3O_8; Jeyagopal *et al.,* 1996) and intensive exploratory drilling by Atomic Minerals Directorate (AMD) have resulted in delineation of substantial uranium deposit in Koppunuru-Chenchu colony area, Guntur district, Andhra Pradesh. In this sector, correlatable uranium mineralization has been intercepted in three sub-horizontal lodes, two of which are restricted to the upper quartz arenite while the third lode is recorded in the basal conglomerate occasionally transgressing to basement granitoids (Verma *et al.,* 2011). Integrated studies have shown that basement granitoids with high intrinsic uranium (19 ppm; U/Th ratio 3.80; n = 30) are the main source of uranium in the system. This uranium was released during the basement reactivation and subsequently remobilized and concentrated along suitable structural locales, particularly along N-S to NNE-SSW trending post-depositional faults/fractures in Banganapalle sediments (Gupta *et al.,* 2009). The mineralisation was accentuated due to the presence of porous and permeable medium *viz.,* quartz arenite and conglomerate facies allowing free flow of mineralised solutions. The presence of suitable reductants like sulphides and carbonaceous matter in host rocks has favoured the precipitation and fixation of uranium (Gupta *et al.,* 2010; Jeyagopal *et al.,* 2011). Discrete primary (pitchblende and coffinite) and secondary (uranophane, phosphouranylite and metazeunerite) U-minerals have been identified from the ore lodes.

Integration of field surface and sub-surface geological and radiometric data together with laboratory data including petromineralogy and chemical data have given substantial insight about the mineralisation pattern in study area. Synthesis of chemical attributes shows insignificant correlation of uranium with major oxides and minor/trace elements (except Pb) in both the host lithofacies *i.e.* conglomerate and quartz arenite. This feature points towards minimum/insignificant role of mineralogy and geochemistry in the distribution pattern of uranium in these lithofacies. However, the strong positive correlation of U and Pb in the sediments indicates radiogenic nature of Pb. Negative correlation of uranium with thorium and high U/Th ratio (Table 2) suggest enrichment of uranium in the sediments due

to tectonic and hydrothermal activities. This is apparent from the surface geological as well as lithological details of subsurface borehole cores showing the presence of uranium anomalies along the fractures, fine veins, cavities and grain boundaries. Uranium mineralisation is also influenced by various alteration phenomenons such as ferrugination, chloritization and kaolinisation as evident from higher concentrations of uranium in association with these alterations. Based on above mentioned features, it can be concluded that uranium mineralisation is predominantly fracture-controlled and epigenetic type in the western part of Palnad sub-basin.

Acknowledgements

The authors are thankful for analytical support from various laboratories of Atomic Minerals Directorate for Exploration and Research (AMD).

References

Armstrong-Altrin, J.S., Lee, Y.I., Verma, S.P. and Ramasamy, S. (2004). Geochemistry of sandstones from the Upper Miocene Kudankulam formation, southern India: Implications for provenance, weathering and tectonic setting. Jour. Sed. Res., v.74, pp.285-297.

Basu, Himadri, Hanumanthappa, D., Saravanan, B., Harikrishnan, T., Rengarajan, M., Bhagat, S. and Mahendra Kumar, K. (2008). Uranium Mineralisation in the Mesoproterozoic Banganapalle Formation near Nagayapalle, Cuddapah basin, Andhra Pradesh., Expl. Res. Atom. Miner., v.18, pp.77-86.

Bhatia, M.R. (1983). Plate tectonics and geochemical composition of sandstones. Jour. Geol., v.91, pp.611-627.

Clark, L.A. (1987). Near surface lithogeochemical haloas an aid to discovery of deeply buried unconformity type uranium deposits, Athabasca basin, Canada. Jour. Geochem. Expl., v.28, pp.71-84.

Condie, K.C. (1993). Chemical composition and evaluation of upper continental crust: contrasting results from surface samples and shales. Chem. Geol., v.104, pp.1-37.

Condie, K.C., Boryta, M.D., Liu, J. and Quian, X. (1992). The origin of Khondalites: geochemical evidence from the Archean to Early Proterozoic granulite belt in the North China Craton. Precamb. Res., v.59, pp.207-223.

Cox, R., Lowe, D.R. and Cullers, R.L. (1995). The influence of sediment recycling and basement composition on evolution of mudrock chemistry in the south western United States. Geochim. Cosmochim. Acta, v.59, pp.2919-2940.

Crawford, A.R. and Compston, W. (1973). The age of the Cuddapah and Kurnool Systems, southern India. Jour. Geol. Soc. Australia, v.19(4), pp.453-464.

Dabard, M.P. (1990). Lower Brioverian formations (Upper Proterozoic) of the Armorican Massif (France): geodynamic evolution of source areas revealed by sandstone petrography and geochemistry. Sed. Geol., v.69, pp.45-58.

Dutt, N.V.B.S. (1975). Geology of the Kurnool System of rocks in Cuddapah and the southern part of Kurnool district. Rec. Geol. Surv. India, v.87, pp.540-604.

Fedo, C.M., Nesbitt, H.W. and Young, G.M. (1995). Unraveling the effects of potassium metasomatism in sedimentary rocks and paleosols, with implications for weathering conditions and provenance. Geology, v.23(10), pp.921-924.

Fedo, C.M., Young, G.M., Nesbitt, H.W. and Hanchar, J.M. (1997a). Potassic and sodic metasomatism in the southern province of the Canadian Shield: evidences from the Palaeoproterozoic Serpent Formation, Huronian Supergroup, Canada. Precamb. Res., v.84, pp.17-36.

Fedo, C.M., Young, G.M. and Nesbitt, H.W. (1997b). Paleoclimatic control on the composition of the Palaeoproterozoic Serpent Formation, Huronian Supergroup, Canada: a greenhouse to icehouse transition. Precamb. Res., v.86, pp.210-223.

Gupta, Shekhar, Deshpande, M.S.M., Jeyagopal, A.V., Umamaheswar, K. and Maithani, P.B. (2009). Uranium mineralization associated with Upper Proterozoic Palnad Sub-basin of the Cuddapah basin in Koppunuru Area, Guntur District, Andhra Pradesh: A Metallogenic Study. 2nd International Conference on 'Precambrian Continental Growth and Tectonism' (PCGT-2009), Jhansi, India.

Gupta, Shekhar, Vimal, Rajiv, Banerjee, Rahul, Ramesh Babu, P.V. and Maithani, P.B. (2010). Sedimentation pattern and Depositional Environment of Banganapalle Formation in South Western Part of Palnad Sub-basin, Guntur District, Andhra Pradesh. Gond. Geol. Mag., Spl. Vol.12, pp.59-70.

GSI (1981). Explanatory brochure on Geological and Mineral Map of Cuddapah Basin (1:250000), pp.1-21.

GSI (2001). Geological and mineral map of Andhra Pradesh (1:500000). Geol. Surv. India, Hyderabad.

Herron, M. M. (1988). Geochemical classification of terrigenous sands and shales from core or log data. Jour. Sed. Pet., v.58(5), pp.820-829.

Jeyagopal, A.V., Deshpande, M.S.M., Gupta, Shekhar, Ramesh Babu, P.V., Umamaheswar, K. and Maithani, P.B. (2011). Uranium mineralization and association of carbonaceous matter in Koppunuru Area, Palnad Sub-basin, Cuddapah basin, Andhra Pradesh. Ind. Mineral., v.45(1), pp.100-111.

Jeyagopal, A.V., Kumar, P. and Sinha, R.M. (1996). Uranium mineralization in the Palnad Sub-basin, Cuddapah Basin, Andhra Pradesh, India. Curr. Sci., v.71(2), pp.957-959.

Karuppan, V.M., Gupta, Shekhar, Rajgopalan, V., Sarbajna, C., Nayak, S. and Shivkumar, K. (2010). Trace Element Distribution in Radioactive Banganapalle Quartzite from Koppunuru Area, Guntur District, Andhra Pradesh, India. Jour. App. Geochem., v.12(3), pp.428-438.

Latha, A., Gupta, Shekhar and Maithani, P.B. (2010). Potential of Pebbly Arenite hosted Uranium Mineralisation at Koppunuru, Guntur District, Andhra Pradesh. 2nd International conference organized by IGCAR, INS and IAEA on "Asian Nuclear Prospects 2010", Chennai, India.

Latha, A., Gupta, Shekhar, Umamaheswar, K. and Maithani, P.B. (2008). Petrological Characterization of uranium bearing host rocks of

Koppunuru, Guntur District, A. P. National workshop "Emerging Geological Concepts on Exploration and Exploitation of Resources " Hyderabad, India, pp.47-48.

Lakshminarayana, G., Bhattacharjee, S. and Kumar, A. (1999). Palaeocurrents and depositional setting in the Banganapalle Formation, Kurnool Sub-basin, Cuddapah basin, Andhra Pradesh. Jour. Geol. Soc. India, v.53(2), pp.255-259.

Lakshminarayana, G., Bhattacharjee, S. and Ramanaidu, K.V. (2001). Sedimentation and stratigraphic framework in the Cuddapah basin. Geol. Surv. Ind. Spl. Pub. No.55, pp.31-58.

Lindsey, D.A. (1999). An evaluation of alternative chemical classifications of sandstones. U.S.G.S. Open File Report 99-34, 23p.

Nagaraja Rao, B.K., Rajurkar, S.T., Ramalinga Swamy, G. and Ravindar Babu, B. (1987). Stratigarphy, structure and evolution of the Cuddapah Basin. Mem. Geol. Soc. India, No.6, pp. 33-86.

Nagarajan, R., Armstrong-Altrin, J.S., Nagendra, R., Madhavraju, J. and Moutie, J. (2007). Petrography and Geochemistry of Terrigenous Sedimentary Rocks in the Neoproterozoic Rabanpalli Formation, Bhima Basin, Southern India: Implications for paleoweathering conditions, provenance and source rock composition. Jour. Geol. Soc., v.70, pp.297-312.

Nageswara Rao, P., Som, A., Perumal, T., Maithani, P.B., Saxena, V.P. and Sinha, R.M. (2005). Proterozoic unconformity related uranium occurrence around Rallavagu Tanda, Palnadu Sub-basin, Andhra Pradesh. Jour. Geol. Soc. India, v.66, pp.11-14.

Natarajan, V. and Rajagopalan Nair, S. (1977). Post-Kurnool thrust and other structural features in the northeastern part of the Palnad basin, Krishna district, Andhra Pradesh. Jour. Geol. Soc. India, v.18(3), pp.111-116.

Naqvi, S.M., Sawarkar, R.H., Subba Rao, D.V., Govil, P.K. and Gnaneswar Rao, T. (1988). Geology, Geochemistry and Tectonic Setting of Archean greywackes from Karnataka Nucleus, India. Precamb. Res., v.39, pp.193-216.

Nesbitt, H.W. and Young, G.M. (1982). Early proterozoic climates and Plate motions inferred from element chemistry of Lutites. Nature, v.299, pp.715-717.

Nesbitt, H.W. and Young, G.M. (1984). Prediction of some weathering trends of plutonic and volcanic rocks based on thermodynamic and kinetic considerations. Geochim. Cosmochim. Acta, v.48, pp.1523-1534.

Nesbitt, H.W. and Young, G.M. (1989). Formation and diagenesis of weathering profiles. Jour. Geol., v.97, pp.129-147.

Nesbitt, H.W. and Young, G.M., McLennan, S.M. and Keays, R.R. (1996). Effects of chemical weathering and sorting on the petrogenesis of silliciclastic sediments, with implications for provenance studies. Jour. Geol., v.104, pp.525-542.

Nesbitt, H.W., Fedo, C.M., Young, G.M. (1997). Quartz and feldspar stability, steadyand non-steady-state weathering, and petrogenesis of siliciclastic sands and muds. Jour. Geol., v.105, pp.173-191.

Pettijohn, F.J., Potter, P.E. and Siever, R. (1972). Sand and sandstone. Springer-Verlag, New York, 618p.

Potter, P.E. (1978). Petrology and Chemistry of modern big river sands. Jour. Geol., v.86, pp.423-449.

Ramakrishnan, M. and Vaidyanadhan, R. (2008). Geology of India (Vol. 1). Geol. Soc. India, Banglore, 556p.

Ramam, P.K. and Murty, V.N. (1997). Geology of Andhra Pradesh. Geol. Soc. India, Bangalore, 245p.

Raza, M., Cashhyap, S.M. and Khan, A. (2002). Geochemistry of Mesoproterozoic lower Vindhyan shales from Chittaurgarh, southern Rajasthan and its bearing on source rock composition, paleoweathering conditions and tectonosedimentary environments. Jour. Geol. Soc. India, v.60, pp.505-518.

Roser, B.P. and Korsch, R.J. (1986). Determination of tectonic setting of sandstone- mudstone suites using SiO_2 content and K_2O/Na_2O ratio. Jour. Geol., v.94, pp.635-650.

Roser, B.P. and Korsch, R.J. (1988). Provenance signatures of sandstone-mudstone suites determined using discriminant function analysis of major element data. Chem. Geol., v.67, pp.119-139.

Saha, D. and Chakraborty, S. (2003). Deformation pattern in the Kurnool and Nallamalai Groups in the northeastern part (Palnad area) of the Cuddapah basin, south India and its implication on Rodinia/Gondwana tectonics. Gond. Res., v.6(4), pp.573-583.

Sivaji, K. and Rao, K.R.P. (1989). Sedimentological studies of Banganapalle Conglomerate in connection with the assessment of diamond resources. Rec. Geol. Surv. India, v.122(5), pp.51-54.

Sopuck, V.J., De Carle, A., Wray, E.M. and Cooper, B. (1983) Application of lithogeochemistry in search for unconformity type uranium deposit in the Athabasca Basin. *In:* E.M. Cameron (Ed.) Uranium Exploration in Athabasca Basin, Sasskatchewan, Canada. Geol. Surv. Canada, Paper 82-11, pp.191-205.

Suttner, L.J. and Dutta, P.K. (1986). Alluvial Sandstone Composition and Paleoclimate, I. Framework Mineralogy. Jour. Sed. Petrol., v.56(3), pp.329-345.

Taylor, S.R. and McLennan, S.M. (1985). The continental crust: its composition and evolution. Blackwell, Oxford, U.K., 349p.

Verma, M.B., Gupta, Shekhar, Singh, R.V., Latha, A., Maithani, P.B. and Chaki, A. (2011). Ore body characterization of Koppunuru uranium deposit in Palnad sub-basin, Guntur district, Andhra Pradesh. Ind. Mineral., v.45(1), pp.51-60.

Vijayam, B.E. and Reddy, P.H. (1976). Tectonic framework of sedimentation in the western part of the Palnad basin, Andhra Pradesh. Jour. Geol. Soc. India, v.17, pp.439-448.

Wanders, A.M., Bradshaw, J.D., Weaver, S., Mass, R., Ireland, T. and Eby, N. (2004). Provenance of the Sedimentary Rakaia sub- terrane, Torlesse Terrane, South Island, New Zealand: the use of igneous clast compositions to define the source. Sed. Geol., v.168, pp.193-226.